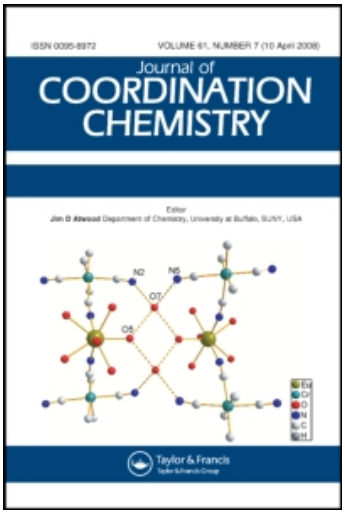

Journal of Coordination Chemistry
Publication details, including instructions for authors and subscription information:
http://www.informaworld.com/smpp/title~content=t713455674

Two supramolecular compounds based on cage-like polyoxovanadates: syntheses, crystal structures, and characterizations

Shu-Yun Shi[ab]; Yan Chen[a]; Bo Liu[b]; Yu-Kun Lu[a]; Jia-Ning Xu[a]; Xiao-Bing Cui[a]; Ji-Qing Xu[a]
[a] Department of Chemistry, College of Chemistry and State Key Laboratory of Inorganic Synthesis and Preparative Chemistry, Jilin University, Changchun 130023, China [b] College of Chemistry, Jilin Normal University, Siping 136000, China

To cite this Article Shi, Shu-Yun , Chen, Yan , Liu, Bo , Lu, Yu-Kun , Xu, Jia-Ning , Cui, Xiao-Bing and Xu, Ji-Qing(2009) 'Two supramolecular compounds based on cage-like polyoxovanadates: syntheses, crystal structures, and characterizations', Journal of Coordination Chemistry, 62: 18, 2937 — 2948
To link to this Article: DOI: 10.1080/00958970902962238
URL: http://dx.doi.org/10.1080/00958970902962238

Journal of Coordination Chemistry
Vol. 62, No. 18, 20 September 2009, 2937–2948

Two supramolecular compounds based on cage-like polyoxovanadates: syntheses, crystal structures, and characterizations

SHU-YUN SHI†‡, YAN CHEN†, BO LIU‡, YU-KUN LU†, JIA-NING XU†, XIAO-BING CUI*† and JI-QING XU*†

†Department of Chemistry, College of Chemistry and State Key Laboratory of Inorganic Synthesis and Preparative Chemistry, Jilin University, Changchun 130023, China
‡College of Chemistry, Jilin Normal University, Siping 136000, China

(*Received 15 December 2008; in final form 6 February 2009*)

Two supramolecular compounds $[Fe(2,2'\text{-bipy})_3]_2[V^V_7V^{IV}_9O_{38}(Cl)]\cdot 4.67H_2O$ (**1**) and $[Ni(enMe)_3]_2[H_4V^V_5V^{IV}_{10}O_{36}(Cl)]\cdot 2H_2O$ (**2**) have been prepared under hydrothermal conditions and characterized by elemental analyses, IR, TGA, ESR, magnetic properties, and single crystal X-ray diffraction analyses. Crystal data for **1**: tetragonal, $I\text{-}42d$, $a = 13.6043(19)$, $b = 13.6043(19)$, $c = 50.544(10)$ Å, $V = 9354(3)$ Å^3; for **2**: hexagonal, $P6(3)/m$, $a = 12.6046(12)$, $b = 12.6046(12)$, $c = 22.563(5)$ Å, $V = 3104.4(7)$ Å^3. Compound **1** is constructed from cations $[Fe(2,2'\text{-bipy})_3]^{3+}$, polyoxovanadates $[V^V_7V^{IV}_9O_{38}(Cl)]^{6-}$, and water molecules. Compound **2** is composed of cations $[Ni(enMe)_3]^{2+}$, clusters $[H_4V^V_5V^{IV}_{10}O_{36}(Cl)]^{8-}$, and water molecules. There are hydrogen-bonding interactions between polyoxovanadates, organic moieties, and/or water molecules in **1** and **2**, forming different 2-D layered networks.

Keywords: Crystal structure; Hydrothermal synthesis; Polyoxovanadates; Hydrogen bonds; Supramolecular framework

1. Introduction

In the past 30 years supramolecular chemistry has developed at a tremendous rate, driven by the growing knowledge regarding synthetic and characterization methods for complex structures [1]. The directed assembly of supramolecular arrays from discrete molecular building blocks is of significant interest with potential applications in catalysis, molecular electronics, sensor design, and optics [2, 3]. In construction of supramolecular materials, one strategy is using low-dimensional building blocks to extend to high-dimensional networks through weak intermolecular interactions, including hydrogen-bonding, $\pi\cdots\pi$ stacking, and van der Waals interactions, etc.

*Corresponding authors. Email: cuixb@mail.jlu.edu.cn; xjq@mail.jlu.edu.cn

Journal of Coordination Chemistry
ISSN 0095-8972 print/ISSN 1029-0389 online © 2009 Taylor & Francis
DOI: 10.1080/00958970902962238

The hydrogen bond is the most familiar organizing force in supramolecular assemblies by virtue of its strength and directionality to control short-range packing [4].

The spherical surface of POMs gives an opportunity for hydrogen bonds and extensive efforts have focused on the design and assembly of such kind of supramolecular architectures [5, 6].

Usually, POMs are based on early transition metals such as V, Mo, W, Nb, or Ta, or mixtures of these elements [7], and polyoxovanadates, especially mixed-valence ones, form a prominent subclass due to their topological structures and rich electronic and magnetic properties [8, 9]. A charming feature of polyoxovanadates is the occurrence of different types of polyhedra ($\{VO_4\}$, $\{VO_5\}$, and $\{VO_6\}$), of which the $\{VO_5\}$ pyramids with partly or fully reduced V^{IV} polymerize into shell or cage clusters which have topological similarities to fullerenes and structural relations to layers of V_2O_5 [10, 11].

We are interested in assembly of polyoxovanadate-based supramolecular hybrid complexes containing transition metal coordination subunits, for such complexes may exhibit interesting supramolecular structures [12, 13]. As a continuous effort on polyoxovanadate clusters [12], we succeeded in synthesizing two new POM-based supramolecular compounds, $[Fe(2,2'\text{-bipy})_3]_2[V_7^V V_9^{IV} O_{38}(Cl)] \cdot 4.67H_2O$ (**1**) and $[Ni(enMe)_3]_2[H_4V_5^V V_{10}^{IV} O_{36}(Cl)] \cdot 2H_2O$ (**2**), and this article deals with syntheses and structures of **1** and **2**. The crystal structure analyses reveal that the clusters, metal-organic coordination complexes, and/or water molecules construct high-dimensional supramolecular networks through hydrogen bonds, resulting in 2-D layered structures for **1** and **2**, respectively.

2. Experimental

2.1. *Material and methods*

All chemicals were of reagent grade. C, H, and N elemental analyses were carried out on a Perkin-Elmer 2400 CHN elemental analyzer. Infrared spectra were recorded as KBr pellets on a Perkin-Elmer SPECTRUM ONE FTIR spectrophotometer. TG curves were performed on a Perkin-Elmer TGA-7000 thermogravimetric analyzer in flowing air with a temperature ramp of $10^\circ C\,min^{-1}$. ESR spectra were completed on a Bruker ER 200D-SRC spectrometer.

2.2. *Syntheses*

2.2.1. Synthesis of $[Fe(2,2'\text{-bipy})_3]_2[V_7^V V_9^{IV} O_{38}(Cl)] \cdot 4.67H_2O$ (1). Compound **1** was hydrothermally synthesized in 75% yield (based on V). A mixture of $FeCl_3 \cdot 2H_2O$ (0.46 g, 2.84 mmol), NH_4VO_3 (0.39 g, 3.33 mmol), $H_2C_2O_4 \cdot 2H_2O$ (0.21 g, 1.67 mmol), 2,2′-bipy (0.156 g, 1 mmol), and H_2O (15 mL, 167 mmol) was adjusted to pH = 5 with vigorous stirring and then sealed in a 25 mL Teflon-lined stainless steel autoclave and heated at 160°C for 3 days. After cooling to room temperature, black block crystals were isolated, washed with water, and dried at ambient temperature. Anal. Calcd for $C_{60}H_{57.32}ClFe_2N_{12}O_{42.67}V_{16}$ (%): C, 27.8; H, 2.23; N, 6.49; V, 31.45; Cl, 1.37. Found (%): C, 27.71; H, 2.31; N, 6.54; V, 31.39; Cl, 1.43.

2.2.2. Synthesis of $[Ni(enMe)_3]_2[H_4V^V_5V^{IV}_{10}O_{36}(Cl)]\cdot 2H_2O$ (2). Compound **2** was prepared in the same way (pH = 5, 160°C for 3 days) as that of **1** in 81% yield (based on V), but using $NiCl_2\cdot 6H_2O$ (0.39 g, 1.65 mmol), NH_4VO_3 (0.72 g, 6.15 mmol), enMe (0.36 mL, 4.23 mmol), $H_2C_2O_4\cdot 2H_2O$ (0.24 g, 1.90 mmol), and H_2O (15 mL, 167 mmol) as the reactants. Black block crystals were obtained. Anal. Calcd for $C_{18}H_{67.98}ClN_{12}Ni_2O_{38}V_{15}$ (%): C, 10.94; H, 3.47; N, 8.50; V, 38.65; Cl, 1.83. Found (%): C, 10.86; H, 3.50; N, 8.52; V, 38.57; Cl, 1.79.

2.3. *X-ray crystallography*

The reflection intensity data of **1** and **2** were collected on a Bruker Apex II diffractometer equipped with graphite monochromated Mo-Kα ($\lambda = 0.71073$ Å) radiation at room temperature. A total of 39,018 (4648 unique, $R_{int} = 0.0744$) reflections of **1** ($-1 \le h \le 16, -16 \le k \le 16, -62 \le l \le 62,\ 2.27 < \theta < 26.11$) were measured, while a total of 26,282 (2108 unique, $R_{int} = 0.0790$) reflections of **2** ($-15 \le h \le 15, -15 \le k \le 15, -27 \le l \le 27,\ \ 2.07 < \theta < 26.05$) were measured. Both structures were solved by direct methods and refined using full-matrix least-squares on F^2 using SHELXTL-97 crystallographic software package. Anisotropic thermal parameters were refined for all non-hydrogen atoms except OW1, OW2, and OW3 in **1** and O1w in **2**. All hydrogens of the ligands were placed in geometrically calculated positions and refined with fixed isotropic displacement parameters using a riding model; those of water molecules were not located. A summary of the crystallographic data and structure refinements for **1** and **2** are given in table 1.

Table 1. Crystal data and structure refinement parameters for **1** and **2**.

Compound	**1**	**2**
Empirical formula	$C_{15}H_{14.33}Cl_{0.25}Fe_{0.5}N_3O_{10.67}V_4$	$C_3H_{11.33}Cl_{0.17}N_2Ni_{0.33}O_{6.33}V_{2.5}$
Formula weight	647.85	329.64
Crystal system	Tetragonal	Hexagonal
Space group	*I*-42*d*	*P*6(3)/*m*
Unit cell dimensions (Å)		
a	13.6043(19)	12.6046(12)
b	13.6043(19)	12.6046(12)
c	50.544(10)	22.563(5)
V (Å^3)	9354(3)	3104.4(7)
Z	16	12
D_{Calcd} (kg m^{-3})	1.840	2.116
Absorbance coefficient (mm^{-1})	1.933	2.869
θ range (°)	2.27–26.11	2.07–26.05
Completeness	99.7%	99.9%
F(000)	5119	1964
Crystal size (mm^3)	0.601 × 0.256 × 0.449	0.33 × 0.31 × 0.31
Reflection collected	39,018	26,282
R(int)	0.0744	0.0790
Independent reflections	4648	2108
Goodness-of-fit	0.858	1.082
Final *R* indices [$I > 2\sigma(I)$][a]	$R_1 = 0.0641$, $wR_2 = 0.1877$	$R_1 = 0.0786$, $wR_2 = 0.2346$

[a] $R_1 = \Sigma||F_o| - |F_c||/\Sigma|F_o|$; $wR = [\Sigma w(F_o^2 - F_c^2)_2/\Sigma w(F_o^2)^2]^{1/2}$.

3. Results and discussion

3.1. *Synthesis*

Several well-characterized compounds containing the $\{V_{16}O_{38}\}$ anion but with different numbers of reduced vanadium(IV) sites [13–19] were synthesized with pH values from 4 to 5 except $[\{Cu(1,2\text{-pn})_2\}_7\{V_{16}O_{38}(H_2O)\}_2]\cdot 4H_2O$ [14] (did not report the pH value), $K_{10}[H_2V_{16}O_{38}]\cdot 13H_2O$ [15] (pH = 12–14), and $Ni(en)_3\{V^{IV}_{11}V^{V}_{5}O_{38}Cl[Ni(en)_2]_3\}\cdot 8.5H_2O$ [16] (pH = 9), as for **1** (pH = 5). However, the pH values for compounds containing $\{V_{15}O_{36}\}$ anion [17, 18] range from 5 to 7 except $[NH_3(CH_2)_8NH_3]_3[V_{15}O_{36}(Cl)](NH_3)_6(H_2O)_3$ [20] (pH = 2), $[Cu(enMe)_2]_3[V_{15}O_{36}(Cl)]\cdot 2.5H_2O$ [21] and $(NMe_4)_6[V_{15}O_{36}(Y)]\cdot 4H_2O$ ($Y = Cl^-$ or Br^-) [22] (did not report the pH value), indicating that the reaction conditions for synthesis of $\{V_{15}O_{36}\}$ anion is easier to control than that for $\{V_{16}O_{38}\}$, which was first prepared in 1990 [22]; here, the pH value for **2** (pH = 5) was in the range. Ordinarily, pH is the most important factor for the preparation of POM compounds with minor deviation resulting in different assembly [18]. However, the $\{V_{16}O_{38}\}$ and $\{V_{15}O_{36}\}$ anions for **1** and **2** were synthesized at the same pH (pH = 5), reaction temperature, and reaction time. Therefore, starting reactants play a key role in the syntheses showing that starting reactants significantly influence the self-assembly under hydrothermal conditions. The syntheses of **1** and **2** are summarized in scheme 1.

The $H_2C_2O_4\cdot 2H_2O$ is a universal reducer in mixed-valence polyoxovanadate systems because of its weak reducibility; its presence is crucial to obtain the two products. Attempts to synthesize **1** and **2** without oxalic acid were unsuccessful.

3.2. *Description of crystal structures*

3.2.1. Crystal structure of 1. Single-crystal X-ray diffraction analysis reveals that **1** (figure 1) is built up from $[Fe(2,2'\text{-bipy})_3]^{3+}$ cations, $[V^{V}_{7}V^{IV}_{9}O_{38}(Cl)]^{6-}$ anions (shortened as V16), and lattice water molecules. The V16 polyanion exhibits a shell structure with approximate S_4 symmetry, encapsulating a guest Cl^- at its center. The host shell consists of 16 $\{VO_5\}$ distorted square pyramids sharing edges and corners, of which 16 vanadiums are distributed to the surface of the shell with average radius of 3.54 Å to the central Cl^-. Selected bond lengths and angles are given as table S1 in "Supplemental material". Three kinds of O atoms exist in this cluster, 16 O_t atoms, 2 μ_2-O, and 20 μ_3-O atoms. The V–O bond lengths [V–O_{term}, 1.588(7)–1.622(6) Å; V-μ_2-O, 1.847(5) Å and V-μ_3-O, 1.860(6)–2.156(7) Å] are comparable with reported compounds [13–19].

The BVS [23] value for the iron is 3.28, confirming the oxidation state of Fe in **1**. BVS values of vanadium atoms V(1)–V(4) are 4.56, 4.47, 4.28, and 4.58, respectively, the average value is 4.47, very close to the expected value 4.44 for $V^{V}_{7}V^{IV}_{9}$. The V16 anion is

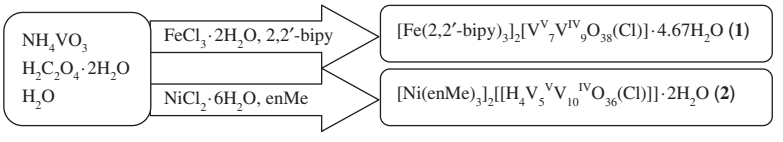

Scheme 1. Schcmatic diagram of the assembly process of **1** and **2**.

assigned as $[V^{V}_{7}V^{IV}_{9}O_{38}Cl]^{6-}$. The manganometric titration of **1** against a standardized $KMnO_4$ solution revealed the presence of nine vanadium(IV) sites per formula unit of **1** [24], consistent with the color of the crystals, results of bond valence sum calculations, crystallographic data, and charge balance requirements. The oxidation state assignments of the V16 cluster in **1** is different from reported polyoxovanadates, such as $[V^{IV}_{11}V^{V}_{5}O_{38}]^{7-}$ [14], $[V^{IV}_{14}V^{V}_{2}O_{38}]^{10-}$ [15], and $[V^{IV}_{7}V^{V}_{9}O_{38}]^{3-}$ [17].

The $[Fe(2,2'\text{-bipy})_3]^{3+}$ in **1** exhibits a typical tri-chelated coordination mode where Fe(III) ion is surrounded by six nitrogens from three bidentate 2,2′-bipy with Fe–N distances 1.943(7)–1.986(9) Å. The two pyridyl rings in each 2,2′-bipy ligand are almost coplanar. Only a few compounds containing iron complexes with POMs were synthesized under hydrothermal conditions with four iron-containing POM systems reported [25, 26], three of which were reported very recently, though the synthesis of iron-based POM materials has been extensively explored under normal bench conditions [26].

There are two kinds of hydrogen bonds in **1** between terminal oxygens of clusters and lattice water molecules and oxygens of clusters and carbons of bipy. As shown in figure 2, a novel 2-D supramolecular array is constructed from V16 clusters and $[Fe(2,2'\text{-bipy})_3]^{3+}$ *via* C–H···O hydrogen bonding interactions. Two $[Fe(2,2'\text{-bipy})_3]^{3+}$ moieties in the supramolecular array could be considered secondary building units (SBU) [27] with Fe–Fe distance of 7.695(3) Å. Each SBU as a linker joins four adjacent V16 clusters through hydrogen bonds between eight carbons from the SBU and eight oxygens from four V16 anions; alternatively, V16 anions are further linked to four SBUs through hydrogen bonds between eight oxygens of the V16 cluster and eight carbons of four SBUs, the distances of hydrogen bonds (C–H···O) is 3.045–3.135 Å. C–H···O plays a key role in forming the supramolecular architecture. In addition, there are hydrogen bonds between oxygens of lattice water molecules and oxygens of V16 clusters with the shortest distance (Ow1–H···O6) 3.005 Å. Synergistic interactions increase the stability of **1**, resulting in new 2-D supramolecular layers.

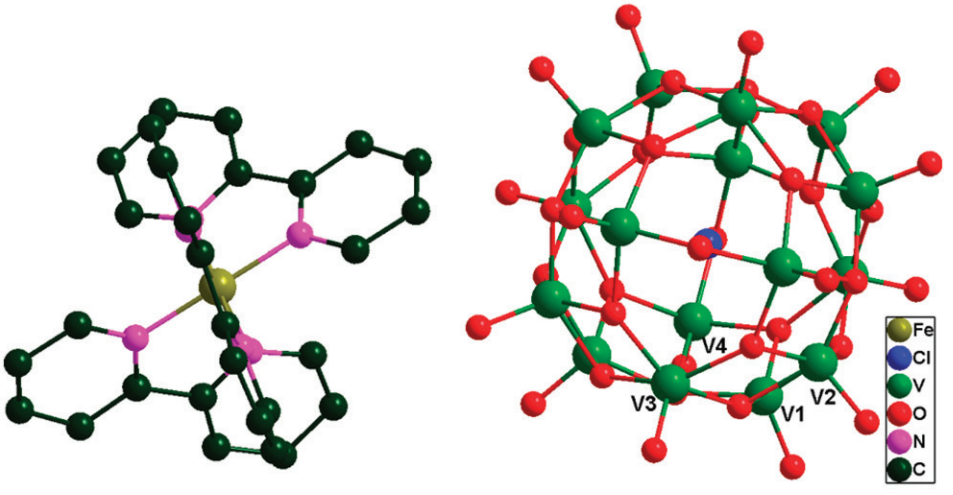

Figure 1. Structure of the polyoxovanadate $[Fe(2,2'\text{-bipy})_3]_2[V^{V}_{7}V^{IV}_{9}O_{38}(Cl)]\cdot 4.67H_2O$.

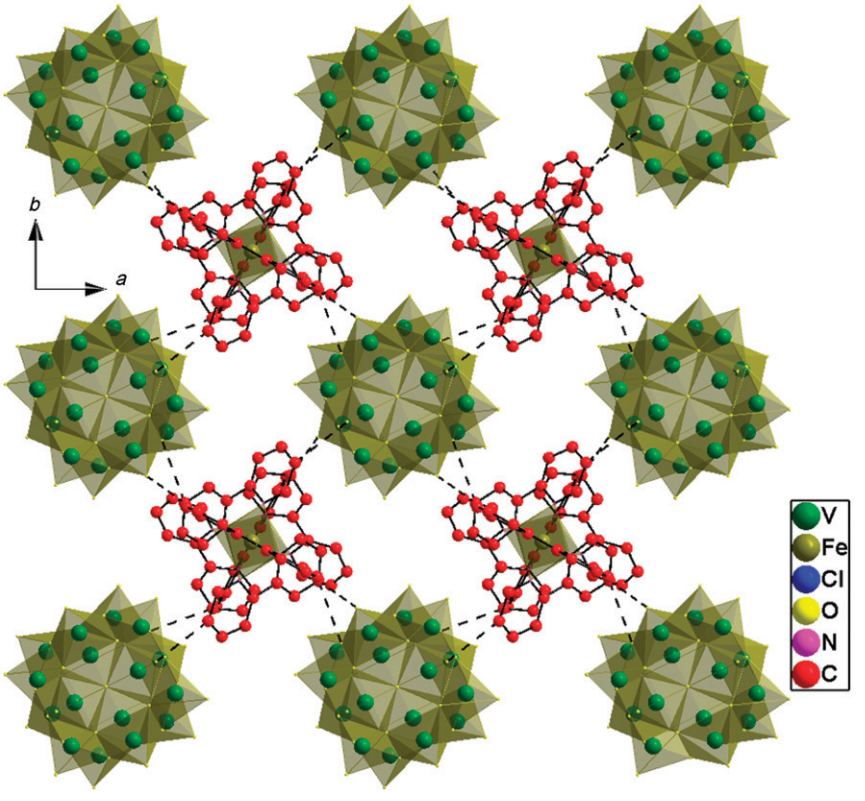

Figure 2. The 2-D layer network structure of **1**.

The array of **1**, a topology-view shown in figure 3, presents a beautiful grid-like structure. Each grid "cell" consists of two V16 clusters and two SBUs, which are connected alternately. The "cell" is further linked into a 2-D layer by sharing "edges". The centroid–centroid distance of the clusters is 13.604(2) Å, while the distance of the SBUs is also 13.604(2) Å.

3.2.2. Crystal structure of 2. As shown in figure 4, **2** consists of $[Ni(enMe)_3]^{2+}$ cations, spherical mixed-valence $[V_{15}O_{36}(Cl)]^{8-}$ polyanions (shortened as V15) and lattice water molecules. The V15 shell with approximate D_{3h} symmetry is constructed from 15 edge- and corner-sharing $\{VO_5\}$ square pyramids with apical and basal V–O bond distances in the range 1.588(6)–2.047(6) Å. The average distance of Cl^- ion from the V atoms of the shell is 3.432 Å. In the V15 anion, oxygens can be divided into three groups, 15 terminal O_t atoms, 3 μ_2-O, and 18 μ_3-O atoms. The V atoms exhibit only one coordination mode, distorted $\{VO_5\}$ square pyramid, which share edges and corners forming shell structure through μ_2- and μ_3-O atoms.

By bond valence sum calculations [23], the Ni atom in **2** has a value of 1.733, indicating that the oxidation state of Ni is 2, while V gives values of 4.674 for V(1), 3.977 for V(2), and 4.591 for V(3). The average oxidation state of V atoms is 4.41, close to the expected value 4.33 for $[V^{V}_{5}V^{IV}_{10}O_{36}(Cl)]^{8-}$. To balance charge, four additional

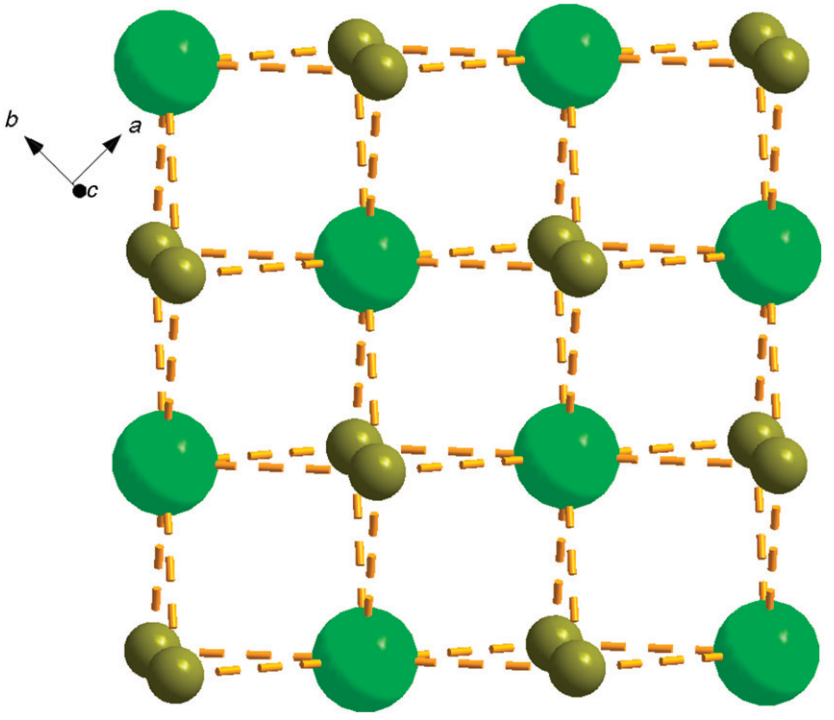

Figure 3. The topology view of the layer of **1**; the big ball represents the V16 and the small ball represents the SBU. The dashed line represents the hydrogen bond.

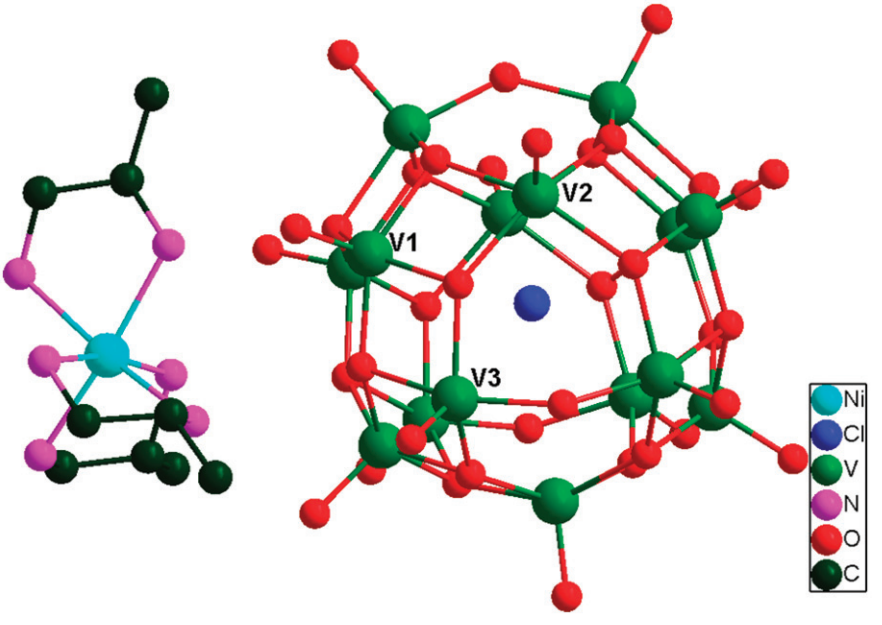

Figure 4. Structure of the polyoxovanadate $[Ni(enMe)_3]_2[H_4V^{V}_5V^{IV}_{10}O_{36}(Cl)] \cdot 2H_2O$.

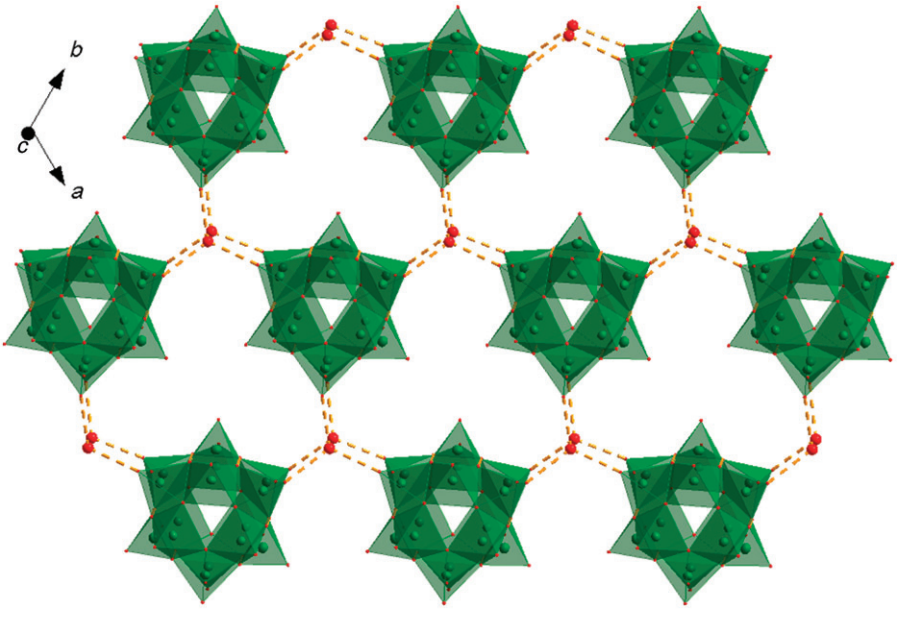

Figure 5. The 2-D layer network structure of **2**.

protons are required, which could not be located experimentally. The manganometric titration of **2** against a standardized $KMnO_4$ solution revealed the presence of 10 vanadium(IV) sites per formula unit of **2** [24], consistent with the color of the crystals, results of bond valence sum calculations, crystallographic data, and charge balance requirements.

The nickel site of $[Ni(enMe)_3]^{2+}$ exhibits a distorted octahedron of six nitrogens from three enMe ligands with Ni–N distances ranging from 2.111(8) to 2.118(8) Å. The closest distance between terminal oxygen atoms of V15 polyoxoanion and carbon atoms coming from enMe is in the range 3.557(1)–3.570(1) Å, indicating interactions of polyoxoanions and cations are very weak (Supplemental material, figure S1).

As shown in figure 5, there is an extensive 2-D supramolecular layer consisting of V15 clusters and lattice water molecules through hydrogen bonds in **2**, with this layer parallel to the crystallographic *ab* plane. Two water molecules in the layer of **2** can be considered as an SBU with the distance of 3.894 Å between the two water molecules, indicating that there is no hydrogen bonding interaction in the SBU. However, each SBU joins three V15 anions through hydrogen bonds between oxygens coming from water molecule of the SBU and six terminal oxygens of three V15 anions; alternatively, each V15 anion connects three adjacent SBUs through hydrogen bonds between six terminal oxygens of the V15 anion and six oxygens from three SBUs, generating large hexagonal channels which are filled with $[Ni(enMe)_3]^{2+}$. The hydrogen bond distances are 2.941(8) Å. In this way, an extensive 2-D supramolecular structure in **2** is formed.

The array of **2** (figure 6) presents a beautiful honeycomb structure. Each honeycomb "cell" consists of three V15 clusters and three SBUs. The "cell" is further linked into a 2-D layer by sharing "edges". The centroid–centroid distance of the clusters is 12.605(1) Å, while the distance of the SBUs is 12.605(1) Å.

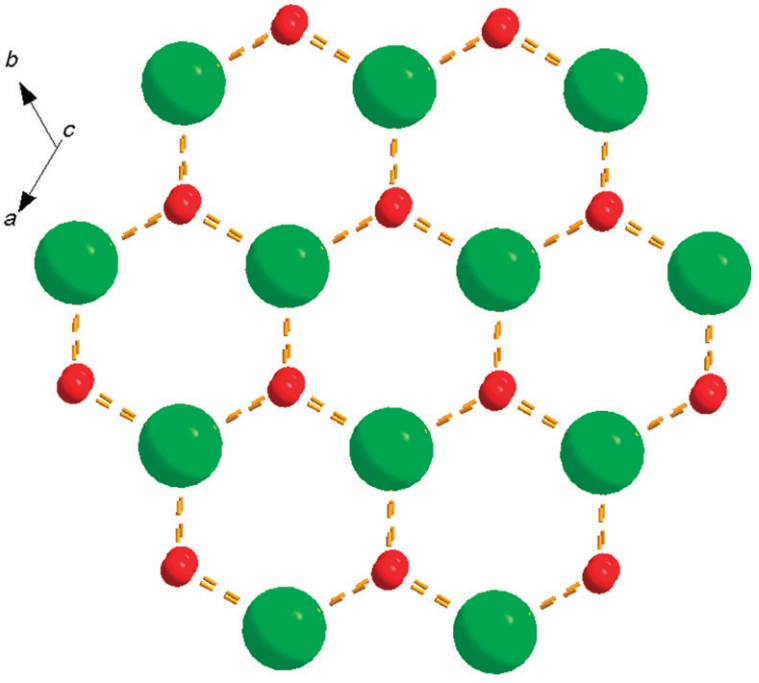

Figure 6. The topology-view of the layer of **1**; the big ball represents the V15 and the small ball represents the SBU. The dashed line represents the hydrogen bond.

3.3. *Characterization of the compounds*

3.3.1. IR spectra of 1 and 2. The IR spectrum of **1** shows intense bands at 980, 773, 734, and 659 cm^{-1} ascribed to the ν(V=O) and ν(V–O–V) vibrations. Compound **1** also possesses a series of bands in the region 1064–1626 cm^{-1} attributed to 2,2′-pyridine. A broad band at 3418 cm^{-1} is associated with water. The infrared spectrum of **2** exhibits stretching bands of NH_2– and CH_2– in the region 2963–3748 cm^{-1}. Bands in the region 1676–1162 cm^{-1} can be attributed to the characteristic vibrations of enMe and a strong band at 974 cm^{-1} can be assigned to V=O bonds. A series of bands in the 515–794 cm^{-1} region are characteristic of ν(V–O–V).

3.3.2. Thermogravimetric analyses. The thermogravimetric analyses were carried out in flowing air with a heating rate of 10°C min^{-1} in the temperature range 25 to 800°C for **1** and **2**, as shown in "Supplementary material". The TGA curve of **1** is similar to that of **2**. Both show weight loss occurring from 25 to 620°C that cannot be divided into individual stages. In the temperature range from 25 to 375°C, both compounds gradually lose weight, while in the range 375 to 475°C, weight loss is rapid. The whole weight loss of **1** is 38.89%, corresponding to loss of six 2,2′-bipy molecules and lattice water molecules per-formula unit, while the total reduction of **2** is 25.32%, attributed to release of four crystal water molecules and six enMe ligands. The observed weight losses (38.89 and 25.19%) are consistent with calculated values (39.30 and 24.51%). There is

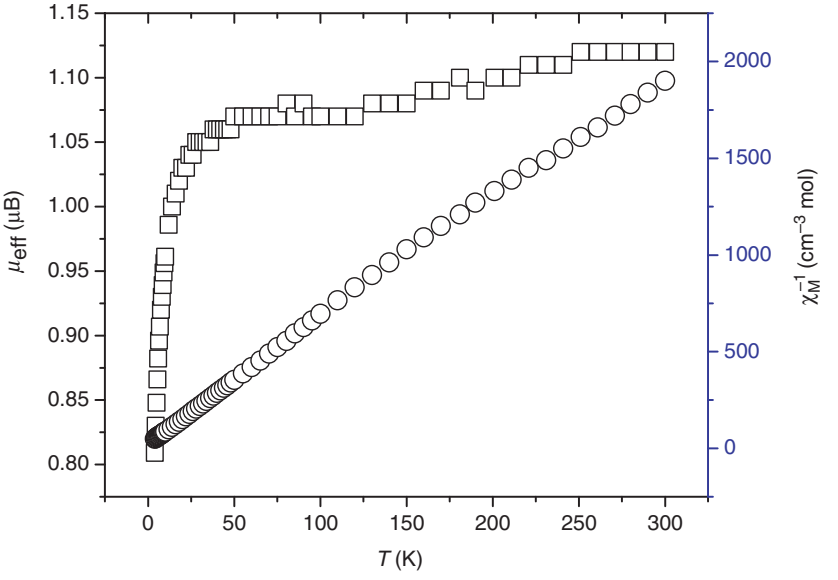

Figure 7. Temperature dependences of the reciprocal magnetic susceptibility χ_M^{-1} (○) and the product μ_{eff} (□) for **1**.

slight increase of weight of **1** and **2** between 535 and 572°C, indicating oxidative processes. Upon further heating, there is no weight change up to 650°C.

3.3.3. ESR spectra for 1 and 2. The ESR spectra (Supplementary material) for **1** and **2** performed at room temperature (298 K) on crystalline samples show Fe^{III} signals with $g = 2.00$ for **1**, and the Ni^{II} signals with $g = 2.11$ for **2**, consistent with valence sum calculations for **1** and **2**.

3.3.4. Magnetic properties of 1 and 2. Preliminary magnetic studies have been performed on powdered samples of **1** and **2** in the range 4–300 K. The temperature dependence of the magnetization was studied in a 1000 Oe field. Figure 7 shows the magnetic behavior of **1** in the form of μ_{eff} *versus* T and χ_M^{-1} *versus* T plots. Upon cooling, μ_{eff} continuously decreases, indicating the presence of antiferromagnetic exchange interactions. The room temperature value of μ_{eff} (1.12 μB) of **1** is smaller than the expected value of μ_{eff} (13.772 μB) for nine uncoupled $S = 1/2$ spins of V^{4+} atoms and two uncoupled $S = 5/2$ spins of Fe^{3+} (assuming $g = 2.00$ for V^{4+} and $g = 2.05$ for Fe^{3+}), indicative of antiferromagnetic coupling. The magnetic data of **1** obey the Curie–Weiss law from 50 to 300 K, and give values $C = 0.16\,\text{emu mol}^{-1}\,\text{K}$ and $\theta = -11.89\,\text{K}$, characteristic of antiferromagnetic interactions of **1**. Unfortunately, it is not easy to fit the experimental magnetic data of this hetero-polymetallic spin system using suitable theoretical models [28].

The magnetic behavior of **2** is more interesting, figure 8, in the form of μ_{eff} *versus* T and χ_M^{-1} *versus* T plots. The μ_{eff} first decreases to 5.58 μB upon cooling from room temperature to 110 K and then increases to 5.71 μB from 110 to 45 K and from 45 to 34 K, the μ_{eff} decreases again to 5.65 μB, from 34 to 14 K, the μ_{eff} increases again to 5.69 μB, from 14 to 4 K, it continuously decreases and finally

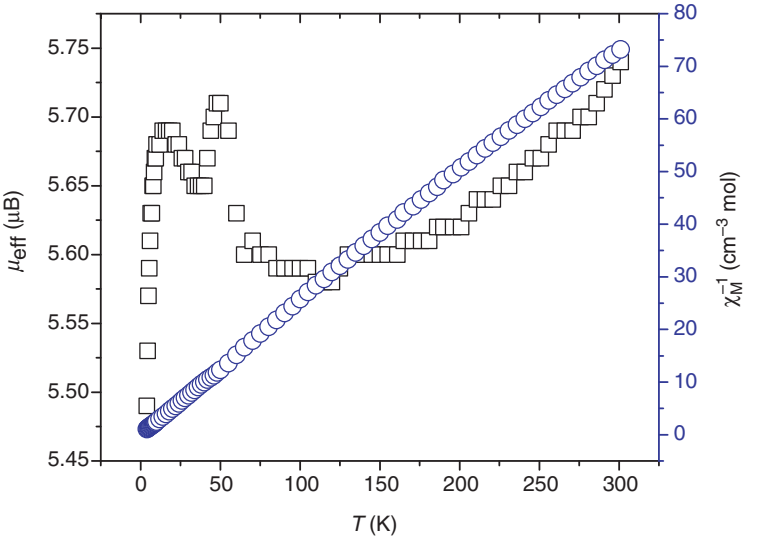

Figure 8. Temperature dependences of the reciprocal magnetic susceptibility χ_M^{-1} (○) and the product μ_{eff} (□) for **2**.

reaches 5.49 μB. Unfortunately, it is not easy to fit the experimental magnetic data of this hetero-polymetallic spin system using suitable theoretical models [28]. The room temperature value of μ_{eff} (5.74 μB) of **2** is smaller than the expected value of μ_{eff} (9.877 μB) of the 10 uncoupled $S = 1/2$ spins of V^{4+} and two uncoupled $S = 1$ spins of Ni^{2+} (assuming $g = 2.00$ for V^{4+} and $g = 2.2$ for Ni^{2+}), indicative of antiferromagnetic coupling. The magnetic data of sample **2** obey the Curie–Weiss law in the 100–300 K temperature region, and give values $C = 4.13\,\text{emu mol}^{-1}\,\text{K}$ and $\theta = -6.57\,\text{K}$, characteristic of antiferromagnetic interactions of **2**.

4. Conclusion

We have prepared and described two cage-like polyoxovanadates with metal-organic complexes, linked *via* various hydrogen bonds, enhancing the stability of the structures.

Supplementary material

CCDC reference numbers: 693798 for **1** and 693799 for **2**.

Acknowledgement

This work was supported by the National Natural Science Foundation of China (Nos 20333070 and 20571032).

References

[1] (a) J.M. Lehn. *Supramolecular Chemistry*, VCH, New York (1995); (b) F. Vögtle. *Supramolecular Chemistry*, Wiley, Chichester (1991); (c) J.-M. Lehn. *Comprehensive Supramolecular Chemistry*, Pergamon, New York (1996).
[2] (a) J.M. Lehn. *Angew. Chem., Int. Ed. Engl.*, **29**, 1304 (1990); (b) J.M. Lehn. *Supramolecular Chemistry*, VCH, Weinheim (1995).
[3] (a) C.N.R. Rao, S. Natarajan, R. Vaidhyanathan. *Angew. Chem., Int. Ed.*, **43**, 1466 (2004); (b) O.M. Yaghi, M. O'Keeffe, N.W. Ockwig, H.K. Chae, M. Eddaoudi, J. Kim. *Nature*, **423**, 705 (2003); (c) B.F. Abrahams, A. Hawley, M.G. Haywood, T.A. Hudson, R. Robson, D.A. Slizys. *J. Am. Chem. Soc.*, **126**, 2894 (2004); (d) J.L.C. Rowsell, O.M. Yaghi. *Microporous Mesoporous Mater.*, **73**, 3 (2004).
[4] S.V. Kolotuchin, E.E. Fenlon, S.R. Wilson, C.J. Loweth, S.C. Zimmerman. *Angew. Chem. Int. Ed.*, **34**, 2654 (1995).
[5] C. Streb, D.-L. Long, L. Cronin. *CrystEngComm.*, **8**, 629 (2006).
[6] (a) V. Coué, R. Dessapt, M. Bujoli-Doeuff, M. Evain, S. Jobic. *Inorg. Chem.*, **46**, 2824 (2007); (b) H. Kumagai, M. Arishima, S. Kitagawa, K. Ymada, S. Kawata, S. Kaizaki. *Inorg. Chem.*, **41**, 1989 (2002).
[7] M.T. Pope. *Heteropoly and Isopoly Oxometalates*, Springer-Verlag, New York (1983).
[8] A. Müller, M.T. Pope, F. Peters, D. Gatteschi. *Chem. Rev.*, **98**, 239 (1998).
[9] A. Müller, R. Sessoli, E. Krickemeyer, H. Bögge, J. Meyer, D. Gatteschi, L. Pardi, J. Westphal, K. Hovemeier, R. Rohlfing, J. Döring, F. Hellweg, C. Beugholt, M. Schmidtmann. *Inorg. Chem.*, **36**, 5239 (1997).
[10] A. Müller, H. Reuter, S. Dillinger. *Angew. Chem., Int. Ed. Engl.*, **34**, 2328 (1995).
[11] W.G. Klemperer, T.A. Marquart, O.M. Yaghi. *Angew. Chem., Int. Ed. Engl.*, **31**, 49 (1992).
[12] W.J. Duan, X.B. Cui, Y. Xu, J.Q. Xu, H.H. Yu, Z.H. Yi, J.W. Cui, T.G. Wang. *J. Solid State Chem.*, **180**, 1875 (2007).
[13] Y.H. Chen, J. Peng, H.Q. Yu, Z.G. Han, X.J. Gu, Z.Y. Shi, E.B. Wang, N.H. Hu. *Inorg. Chim. Acta*, **358**, 403 (2005).
[14] B.Z. Lin, S.X. Liu. *Chem. Commun.*, 2126 (2002).
[15] D.L. Long, D. Orr, G. Seeber, P. Köerler, L.J. Farrugia, L. Cronin. *J. Cluster Sci.*, **14**, 313 (2003).
[16] C.L. Pan, J.Q. Xu, G.H. Li, D.Q. Chu, T.G. Wang. *Eur. J. Inorg. Chem.*, 1514 (2003).
[17] C.D. Zhang, S.X. Liu, B. Gao, C.Y. Sun, L.H. Xie, M. Yu, J. Peng. *Polyhedron*, **26**, 1514 (2007).
[18] B.X. Dong, J. Peng, Y.H. Chen, Y.M. Kong, A.X. Tian, H.S. Liu, J.Q. Sha. *J. Mol. Struct.*, **788**, 200 (2006).
[19] Y.H. Chen, X.J. Gu, J. Peng, Z.Y. Shi, H.Q. Yu, E.B. Wang, N.H. Hu. *Inorg. Chem. Commun.*, **7**, 705 (2004).
[20] T. Drezen, O. Joubert, M. Ganne, L. Brohan. *J. Solid State Chem.*, **136**, 298 (1998).
[21] J.R.D. Debord, R.C. Haushalter, L.M. Meyer, D.J. Rose, P.J. Zapf, J. Zubieta. *Inorg. Chim. Acta*, **256**, 165 (1997).
[22] A. Müller, M. Penk, R. Rohlfing, E. Krickemeyer, J. Döring. *Angew. Chem., Int. Ed.*, **29**, 926 (1990).
[23] I.D. Brown, M. O'Keefe, A. Navrotsky (Eds). *Structure and Bonding in Crystals*, Academic Press, New York (1981).
[24] A. Müller, M. Penk, J. Döring. *Inorg. Chem.*, **30**, 4935 (1991).
[25] S. Chang, C. Qin, E. Wang, Y. Li, X. Wang. *Inorg. Chem. Commun.*, **9**, 727 (2006).
[26] C. Pichon, A. Dolbecq, P. Mialane, J. Marrot, E. Riviére, M. Goral, M. Zynek, T. McCormac, S.A. Borshch, E. Zueva, F. Sécheresse. *Chem. Eur. J.*, **14**, 3189 (2008).
[27] N.L. Rosi, J. Kim, M. Eddaoudi, B. Chen, M. O'Keeffe, O.M. Yaghi. *J. Am. Chem. Soc.*, **127**, 1504 (2005).
[28] O. Khan. *Molecular Magnetism*, VCH, Weinheim, Germany (1993).